

Mechanical Properties and Fracture Behavior of Directionally Solidified NiAl-V Eutectic Composites

SRDJAN MILENKOVIC and RUBENS CARAM

Directional solidification of eutectic alloys has been recognized as promising technique for producing *in situ* composite materials exhibiting balance of properties. Therefore, an *in situ* NiAl-V eutectic composite has been successfully directionally solidified using Bridgman technique. The mechanical behavior of the composite including fracture resistance, microhardness, and compressive properties at room and elevated temperatures was investigated. Damage evolution and fracture characteristics were also discussed. The obtained results indicate that the NiAl-V eutectic retains high yield strength up to 1073 K (800 °C), above which there is a rapid decrease in strength. Its yield strength is higher than that of binary NiAl and most of the NiAl-based eutectics. The exhibited fracture toughness of 28.5 MPa√m is the highest of all other NiAl-based systems investigated so far. The material exhibited brittle fracture behavior of transgranular type and all observations pointed out that the main fracture micromechanism was cleavage.

DOI: 10.1007/s11661-014-2427-6

© The Minerals, Metals & Materials Society and ASM International 2014

I. INTRODUCTION

THERE has been considerable interest in NiAl as a candidate material for high-temperature applications in aerospace engines, largely due to its attractive combination of properties.^[1,2] Beside the high melting temperature [1947 (1674 °C)], it offers exceptional oxidation resistance [up to 1573 K (1300 °C)], moderate density (5.90 g/cm³), high thermal conductivity, and low brittle-to-ductile-transformation-temperature (BDTT). However, like most other intermetallic compounds, NiAl has its share of inherent problems. At room temperature, NiAl suffers from low ductility and poor fracture toughness, while at elevated temperatures exhibits low yield strength and creep resistance. In order to achieve the desirable balance of properties, two approaches have been considered. First one is improving the high-temperature strength by dispersion strengthening and the other, compositing NiAl with continuous-fiber reinforcements as a means of improving both the toughness and the strength.^[2] Although a large volume of work on dispersion strengthening of the NiAl has resulted in improved high-temperature strength and creep resistance, no significant improvements have been made in increasing the low-temperature fracture toughness. Another method of imparting damage tolerance into intrinsically brittle intermetallics is by ductile-fiber^[3] and ductile phase-toughening.^[4,5] A special emphasis has been devoted to

the incorporation of refractory metal or intermetallic (Heusler or Laves) phases through directional solidification (DS) of eutectic alloys. DS eutectics can be considered as natural composites since their structure consists of two or more separate solid phases under normal solidification conditions. The advantages DS eutectics have over single phase intermetallics include an improvement in both strength and toughness by various intrinsic and extrinsic mechanisms, and a natural chemical and mechanical compatibility between the reinforcement and the matrix, which is extremely important feature for high-temperature applications in hostile environments for extended periods of time.

The NiAl forms a number of pseudobinary eutectic systems with either a nominally ductile refractory phase (Cr, Mo, Re, V, W) or with intermetallic phase of the Heusler or Laves type (Hf, Nb, Ti, Ta). Significant progress has been made through this *in situ* composite system approach.^[6–15] From these studies, effects of the type of reinforcement phase on the key properties (fracture toughness and creep strength) can be easily ascertained. It has been shown that the NiAl-Laves phase eutectics exhibit good creep strength compared to other NiAl alloys, but unfortunately have a fracture toughness on the order of 5 MPa√m. However, this value is about average fracture toughness for most polycrystalline NiAl alloys and soft oriented crystals. Therefore, the large increase in creep strength for the NiAl-Laves phase alloys compared to binary NiAl is not gained at the expense of fracture toughness. On the other hand, the NiAl-metal phase alloys exhibit a factor of two or three increase in fracture toughness, but generally possess moderate improvement in creep strength over that of binary NiAl.

Regarding the NiAl-V system, there is only limited information presented in the literature. Pellegrini and Huta^[16] pointed out the existence of pseudobinary

SRDJAN MILENKOVIC, Head, is with the Solidification Processing and Engineering Group, IMDEA Materials Institute, C/Eric Kandel 2, 28906 Getafe, Madrid, Spain. Contact e-mail: srdjan.milenkovic@imdea.org RUBENS CARAM, Professor, is with the Department of Materials Engineering, State University of Campinas, P.O. 6122, 13083-970 Campinas, SP, Brazil, and also with the FEM/UNICAMP, Rua Mendeleev, 200, 13083-860 Campinas, SP, Brazil.

Manuscript submitted February 26, 2014.

Article published online July 9, 2014

eutectic NiAl-V without determining the exact composition. Cotton and Kaufman^[17] studied NiAl-rich hypoeutectic alloys and predicted a limited increase in fracture toughness due to solid solution hardening effects. In that investigation, the microhardness of the vanadium phase nearly triples and becomes greater than that of the NiAl phase for the two phase alloys. Based on this data, the outlook for vanadium as a potential ductile reinforcement was not good despite the high volume fraction of a metallic phase. However, in a sole investigation on the mechanical properties of the NiAl-V eutectic system,^[18] the reported fracture toughness of $32 \text{ MPa}\sqrt{\text{m}}$ was the highest of all NiAl-based eutectics. This surprisingly high value was attributed not only to the high volume fraction of the strengthened V solid solution in conjunction with crack bridging and crack re-nucleation mechanisms, but also to intrinsic toughening of the NiAl phase. In previous investigations on the constitution and solidification behavior of the NiAl-V eutectic by the present authors, the accurate eutectic composition and temperature,^[19] as well as the effect of the composition^[20] and the growth conditions on the microstructure and morphology were reported.^[21] The present work was undertaken to evaluate mechanical properties of a NiAl-V eutectic alloy.

II. EXPERIMENTAL PROCEDURE

The starting materials were Ni, Al, V with the purities 99.99, 99.95, 99.7 wt pct, respectively. The alloys with composition Ni-30.5Al-39V in at. pct were prepared in the form of ~50 g buttons by arc-melting in a water-cooled copper hearth, using a non-consumable tungsten electrode. Each button was melted more than three times and flipped over between each melting to promote homogeneity. The arc-melted ingots were then remelted in a Bridgman furnace and directionally solidified at the growth rate of 1.0 cm/h and thermal gradient of ~100 °C/cm. Ingots were 50 mm long and 10 mm in diameter.

Cylindrical compression specimens were electrical discharge machined from selected ingots. The specimens were 6 mm in diameter by 9 mm in length, with the compression axis parallel to the growth direction. Mechanical properties were measured under both constant velocity conditions and under constant load conditions in universal MTS Test Star II facility at temperatures between 1073 K and 1273 K (800 °C and 1,000 °C). In order to reduce friction, sample surface was lubricated with Molybdenum disulfide. The strain was recorded as the cross head displacement. Constant velocity experiments were used to determine the behavior at fast strain rates, while constant load testing was employed for slower rates. Overlapping steady state stress-strain rate data from the two techniques indicated excellent correlation between constant load and constant rate tests. All testing was performed in air as a secondary check for environmental resistance under load.

The room temperature fracture toughness of the *in situ* composite was also measured by using 3-point

bending technique. Specimens with dimension of $4 \times 8 \times 45 \text{ mm}$ were electrical discharge machined parallel to the growth direction. A notch with an a/w (notch length/specimen width) ratio of 2/5 was cut perpendicular to the growth direction. A fatigue pre-crack was not initiated at the notch tip prior to testing. Bend tests were performed on a servo-hydraulic machine using displacement rate of 0.5 mm/min. Fracture toughness values were calculated using the K -calibration for pure bending. The fracture surfaces of the composite after fracture testing were cut and ultrasonically cleaned before SEM examination. A section near the fracture surface of each specimen was also metallographically prepared in order to investigate the damage mechanisms.

III. RESULTS AND DISCUSSION

A. Initial Microstructure

Although melting in an arc furnace does not permit any control of the solidification process, the resulting morphologies presented a high degree of regularity and uniformity, with an orientation clearly dependent on the direction of heat flux during solidification (Figure 1). Also, the microstructure was fully eutectic without the presence of the primary phases, indicating the solidification occurred within the coupled growth region. Moreover, several variations in the regularity of the microstructure of the same sample were observed. Actually, it was possible to distinguish three different regions, as schematically shown in Figure 1. Region I, located near the top surface of the ingot exhibited coarse eutectic microstructure characterized by equiaxed colonies with predominantly lamellar morphology within cells (Figure 1(b)). As this region was last to solidify, its local solidification time was the lowest, which resulted in a coarse eutectic structure. The region II (Figure 1(c)) showed a columnar microstructure composed of several eutectic grains oriented in the direction of heat extraction. These elongated grains exhibited distinct morphologies depending on the orientation. Finally, region III at the lower surface in contact with the water-cooled copper crucible showed an equiaxed cellular eutectic morphology with much finer lamellar spacing. Lamellae inside the cells were also less oriented and more irregular, as shown in Figure 1(d). Considering that it has been subjected to a high cooling rate, the observed microstructure conforms to the theory of regular eutectic growth that predicts a decrease of the regularity of the structure and eutectic spacing with an increase in the solidification rate.^[22]

The microstructures of the transverse and the longitudinal sections of the directionally solidified NiAl-39V alloy are shown in Figure 2. It may be observed quite regular microstructure with either lamellar or fibrous morphology (Figures 2(a) and (b)). Despite of the growth rate and direction being controlled, a polycrystalline structure was obtained. All grains were oriented parallel to the growth direction, with the regular interphase spacing. In addition to the above microstructural characteristics, several growth defects like layer

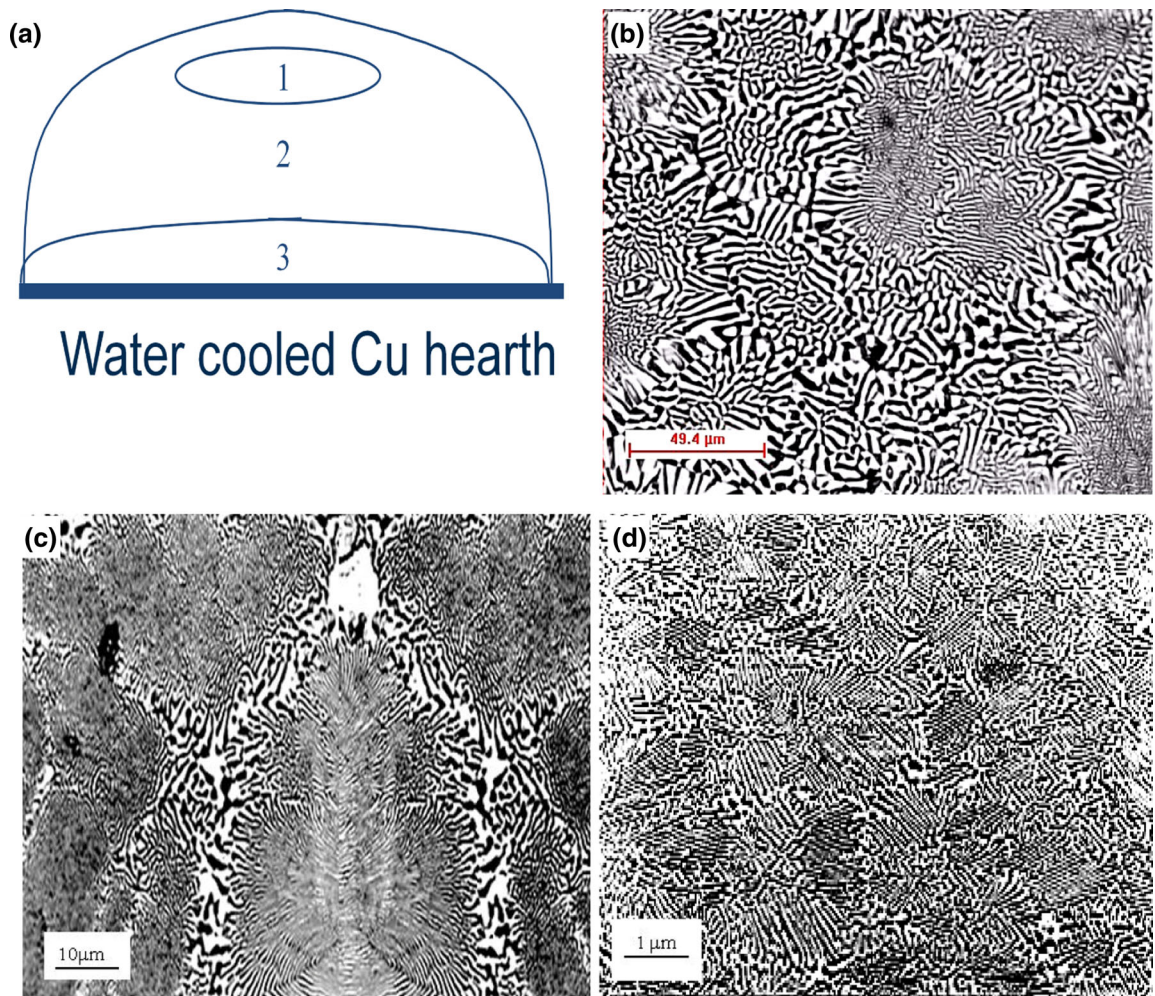


Fig. 1—Microstructure of the arc-melted as-cast samples: (a) schematic of the ingot with three different regions, (b) region I, (c) region II, and (d) region III.

mismatches and lamellar terminations were observed within each grain. As may be seen in Figure 2(c), the lamellae are not continuous but are broken in places, and that these breaks are almost perpendicular to the plane of the lamellae. It may also be observed that the lamellae on either side of such break are slightly shifted with respect to each other. These breaks in the lamellae are known as fault lines. A count of the number of lamellae on either side of a fault line reveals that, in most cases, there is an extra lamella on one side of the fault line, which is called a fault. In the case of fibrous morphology, regularity and uniformity were higher. Figure 2(d) shows two adjacent grains, one exhibiting fibrous morphology, and the other lamellar, even though they have grown under identical conditions. The fact that contiguous grains in directionally solidified alloys often show quite different morphologies is an important observation related to the orientation relationships, whose implication is often missed. Actually, the only explanation for the observed difference in morphology is that the orientation relationships between the phases are different in the two grains. According to Hunt and Chilton,^[23] the preferential

morphology is the one that grows with the least undercooling. In an approximate calculation they showed that the undercooling for rods is less than that for lamellae when the volume fraction of the rod phase (V_A) is less than $\pi (\sigma_L/\sigma_R)^2$, where σ_L is the interphase energy per unit area between the lamellae, and σ_R is the interphase energy per unit area around the rods. Since it is known that during lamellar growth a low energy semi-coherent boundary develops between the lamellae, implies that $\sigma_L \leq \sigma_R$. Therefore, for certain α and β orientations and growth directions, σ_L may be small enough for lamellae to be formed, but for other conditions σ_L will approach σ_R , so that rods are formed. At the longitudinal sections, in much the same way as in a previous case both eutectic morphologies were encountered (Figures 2(e) and (f)). However, the microstructure of NiAl-39V alloy was regular, without any traces of eutectic cells, dendrites, or colonies. The absence of eutectic cells implied that during eutectic growth, solid/liquid interface presented a high level of stability, which is associated with minimal constitutional undercooling. Also, highly regular and dendrite free microstructure indicated that the chemical composition

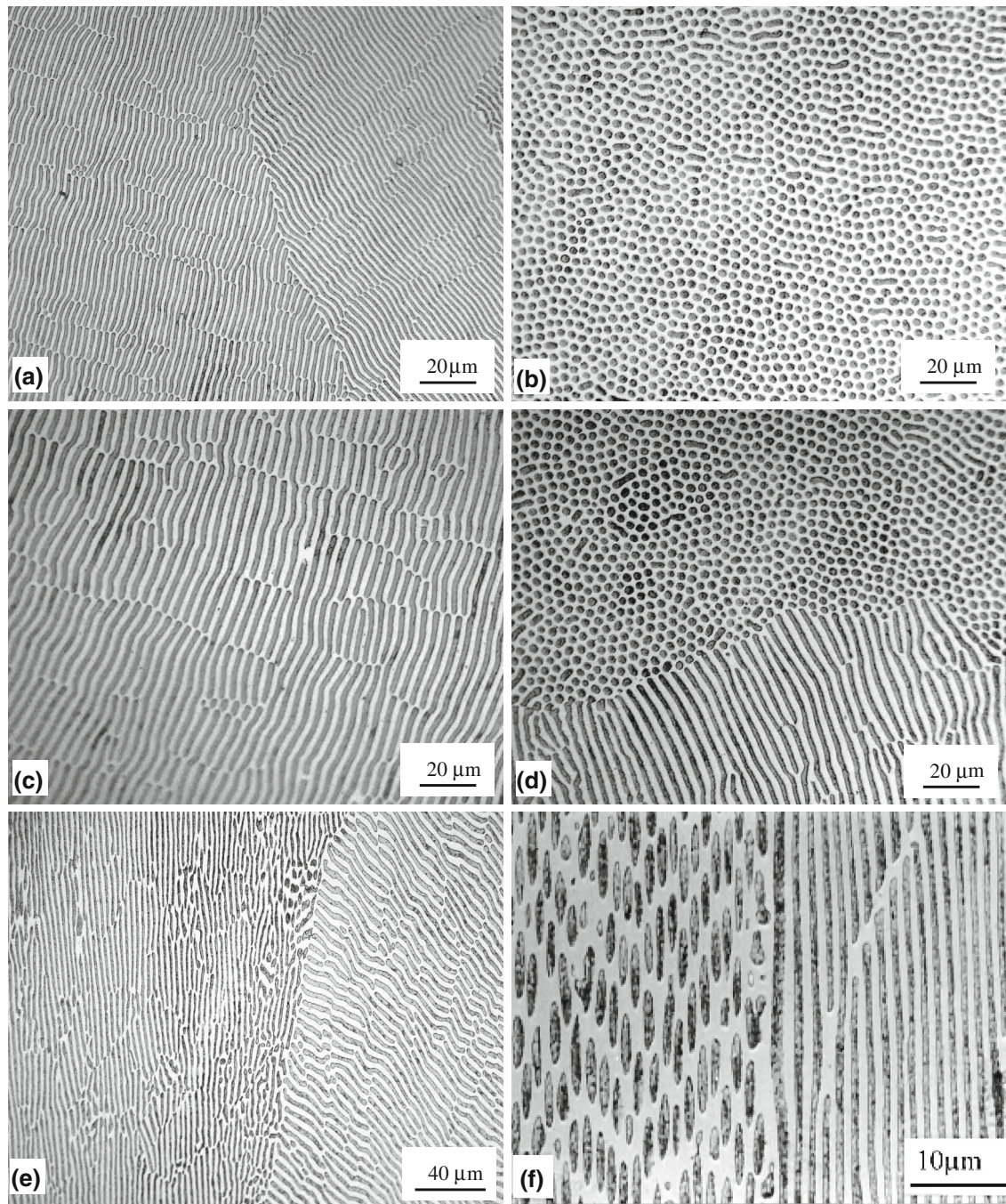


Fig. 2—Microstructure of directionally solidified NiAl-V *in situ* composite: (a) through (d) transverse section and (e) through (f) longitudinal section.

of the alloy matched the eutectic composition exactly. Even a small amount of the primary phase would have perturbed the regularity of eutectic microstructure and have provoked the alteration of the growth direction in its vicinity.

B. Compressive Properties

Figure 3 shows room temperature stress–strain curves of directionally solidified and arc-melted eutectic alloys. It can be noted that the arc-melted alloys present higher yield strength, but lower fracture strain. This can be explained by

the difference in the processing conditions of two alloys. Since the arc-melted alloy was subjected to higher solidification rate and undercooling, produced by water-cooled copper hearth, it exhibited lower grain size and finer lamellar spacing. The lamellar spacing was lower in the arc-melted sample ($\lambda \approx 1 \mu\text{m}$) than in the one solidified directionally ($\lambda \approx 7 \mu\text{m}$). Moreover, in the arc-melted sample the amount of residual stresses in the microstructure is higher. All these factors contributed to higher strength and lower ductility of the arc-melted sample.

Comparing these results with those of NiAl^[1,2,24] (Table I), it can be observed that the eutectic NiAl-V

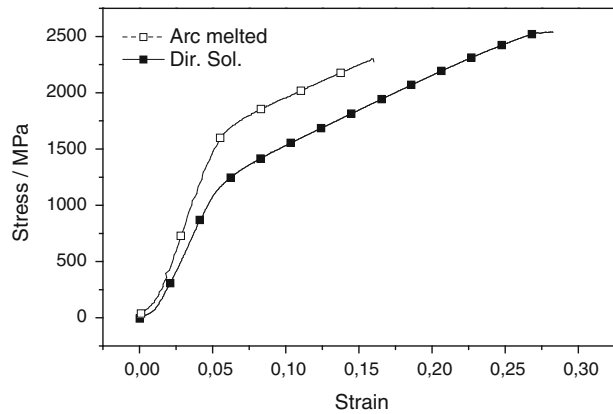


Fig. 3—Stress–strain curves at room temperature of the arc-melted and directionally solidified alloys.

Table I. Yield Strength of NiAl-V Alloys Compared to NiAl Mono- and Poly-crystals

Sample	$\sigma_{0.2}$ (MPa)	σ_m (MPa)	ϵ (Percent)
NiAl-V as-cast	1525.3	2375.7	17.3
NiAl-V Dir. Sol.	1144.0	2075.7	25.2
NiAl $\langle 100 \rangle$ ^[1]	980 to 1400		
NiAl $\langle 110 \rangle$ ^[24]	165 to 190		
Ni-53Al Poly ^[2]	1180		
Ni-49.6Al ^[2]	190		
Ni-43Al ^[2]	800		

exhibits higher yield strength than most of the NiAl single and polycrystals. Only the single crystal with [100] orientation and polycrystalline NiAl rich in Al (Ni-53Al) have higher yield strengths. Similarly, the compressive ductility or the fracture strain of the composite material exhibited higher values than those of polycrystalline and monocrystalline NiAl, except for single crystals with [100] orientation and polycrystalline Ni-53Al.^[2] This is probably a result of the interaction of a brittle phase, the intermetallic compound NiAl, which has high strength but low ductility, with the ductile V phase. Several studies have shown that the incorporation of a ductile phase in an intermetallic matrix can improve its mechanical properties. During the formation and propagation of cracks, ductile phase deforms plastically, consuming much strain energy and therefore contributes to the increased ductility of the material. In this case also the increase in ductility can be attributed to the presence of a ductile phase.

The temperature dependence of the yield stress for the number of eutectic alloys is depicted in Figure 4 and compared with other eutectic alloys^[25,26] (Milenkovic, unpublished results). In all cases, there is a decrease of the yield stress with temperature, showing three different regions. From room temperature to 673 K to 873 K (400 °C to 600 °C) there is a plateau, then a sharp drop in yield strength at intermediate temperatures followed by a region of slight decrease. A sudden drop in yield strength is associated with the change of deformation mechanisms that occur at temperatures around BDTT,

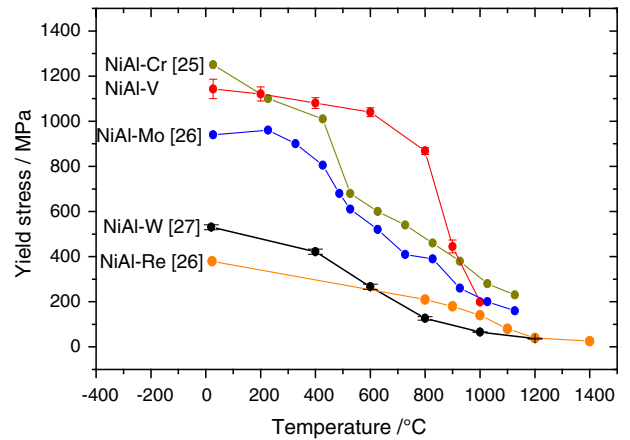


Fig. 4—Temperature dependence of the yield strength of directionally solidified alloys.

which coincide with those of the observed phenomenon. This behavior is more pronounced for binary NiAl, while for eutectic alloys is apparently faster and occurs at slightly higher temperatures. Moreover, at intermediate and high temperatures, all composites exhibit higher limits than the monocrystalline NiAl. In the case of NiAl-V alloy, plateau extends up to 1073 K (800 °C), followed by a sharp drop. The high dependence of the yield strength on the temperature is characteristic for BCC metals. This behavior results from the fact that the recombination of partial dislocations, which is prerequisite for the cross slip and dislocation climb, is thermally activated process. Therefore, with the increase in temperature, the cross slip and dislocation climb are facilitated, resulting in lower yield strength.

For the temperature range of 1073 K to 1273 K (800 °C to 1000 °C), tests were performed with three strain rates to evaluate its effect on the mechanical behavior of the NiAl-V composite. Figure 5 shows typical curves observed. At all test temperatures, an increase in the yield strength with increasing strain rate was noticed. This behavior can be understood by taking into consideration the fact that the increase of the strain rate decreases the time for thermally activated processes. Therefore, the increase in strain rate leads to the same effects as the temperature decrease. Another interesting fact that is related to the influence of strain rate is the shape of the stress–strain curves. For high strain rates of deformation, a rapid hardening to approximately 5 pct strain followed by continuous hardening under almost constant stress was observed. Conversely, at the lowest strain rate, the stress increases rapidly to a peak at a relatively low strain level (~3 pct), followed by a stress in voltage to a constant value. This phenomenon indicates the occurrence of dynamic recovery and/or recrystallization at these conditions.

C. Microhardness

To provide a more complete insight into mechanical properties of the NiAl-V *in situ* composite, microhardness tests were also carried out. The Vickers hardness tests were conducted at room temperature

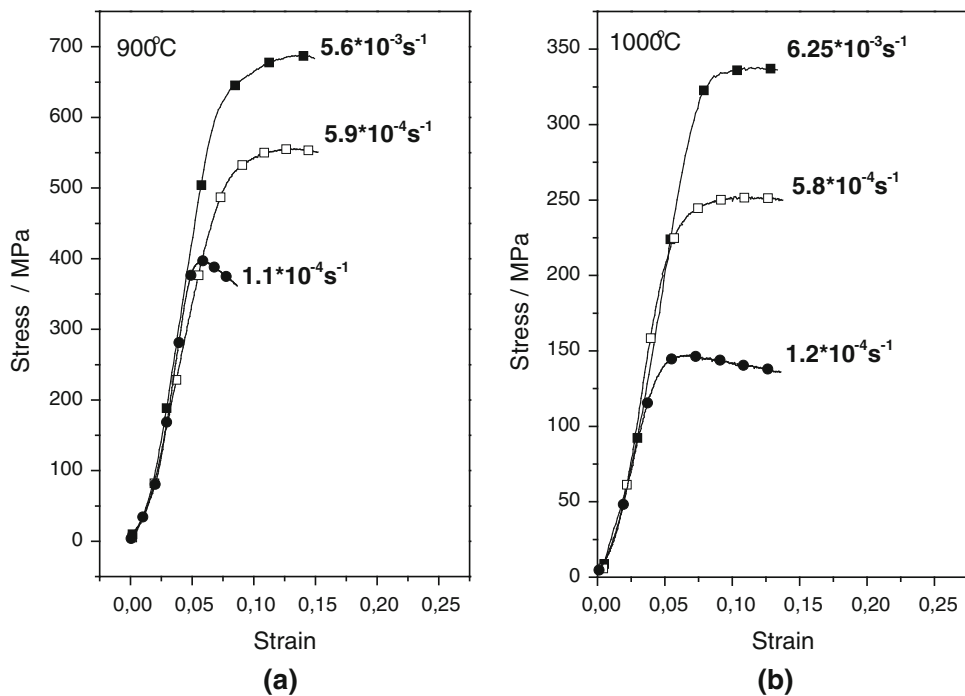


Fig. 5—Influence of the strain rate on the yield strength at (a) 1173 K (900 °C) and (b) 1273 K (1000 °C).

Table II. Microhardness of the NiAl-V Eutectic and its Constituent Phases

Material	This Study	Reference 17
NiAl-V (DS)	408.3	
NiAl-V (AC)	475.5	380 to 414
α V	438	379
β NiAl	501	356
pure V		120
pure NiAl		254

with 50 to 1000 gf load for the eutectic alloy in the as-cast state and after DS and the results are presented in Table II. It can be observed that the microhardness of as-cast sample is greater than in directionally solidified alloys. Due to the high cooling rate involved during electric arc-melting, the microstructure is finer showing lamellar spacings of the order of $1.0 \mu\text{m}$, while the directionally solidified has larger and more regular spacings.

For comparison, the values of pure NiAl and V from Reference 17 are also included. The hardness of the constituent phases were determined in hypo- and hyper-eutectic samples. Analyzing the results, in addition to hardening of the β NiAl phase, a dramatic increase in hardness α phase V was observed. From the fact that the microhardness of α V phase increased more than the hardness of NiAl, it can be concluded that α V phase is much more sensitive to the solution hardening. Furthermore, the two alloys withstood indentations with the higher loads and did not crack even under load of 120 kgf, suggesting good fracture toughness (Figure 6). The hardness values in the literature and those obtained

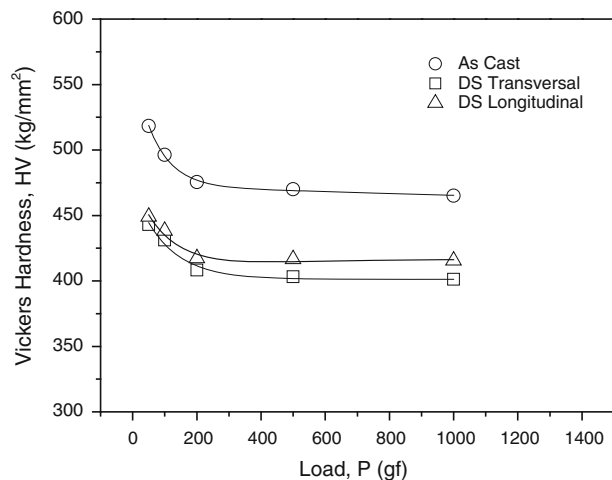


Fig. 6—Microhardness as a function of the applied load.

in this work indicate that the eutectic *in situ* composites exhibit a balance of hardness of their constituent phases. At loads below 200 gf, the indentation size effect was observed.

D. Fracture Behavior

In the three points bending test, the load P was recorded due to the opening of the extensometer (COD). From this diagram, the P_5 load was subsequently used for the calculation of K_P and K_Q , the criteria being adopted in the ASTM E-399.^[29] Considering that the bending tests were conducted without fatigue induced pre-crack, the results of fracture toughness values

obtained correspond to the K_Q value rather than K_{IC} . The fracture toughness K_Q of the NiAl-V composite material was $28.64 \pm 0.28 \text{ MPa}\sqrt{\text{m}}$. This value is close to the result of Joslin *et al.*^[18] who obtained the value of $32.9 \text{ MPa}\sqrt{\pm 3.6 \text{ m}}$. As mentioned previously, the incorporation of a ductile phase, an intermetallic matrix can enhance the mechanical properties of an essentially

brittle material. During the formation and propagation of cracks, ductile phase deforms plastically, consuming much strain energy and therefore contributes to the increased ductility of the material. Furthermore, the ductile phase is presented as an obstacle to crack propagation by diverting broken, thus contributing to the improvement of the fracture toughness of the

Table III. Fracture Toughness of NiAl-Based Eutectic Composites

Eutectic System	Fracture Toughness, K_Q (MPa $\sqrt{\text{m}}$)	Minor Phase V_f (Percent)	Morphology	Reference
NiAl-9Mo	9.5	14	fibrous	[27]
NiAl-9Mo	15	14	fibrous	[28]
NiAl-34Cr	20	34	fibrous	[28]
NiAl-28Cr-6Mo	22	34	lamellar	[28]
NiAl-15,5 Ta	5	47	lamellar	[18]
NiAl-16,5Nb	5	48	lamellar	[18]
NiAl-40V	32	36	lamellar	[18]
NiAl-39V	28.6	36	lamellar	this study

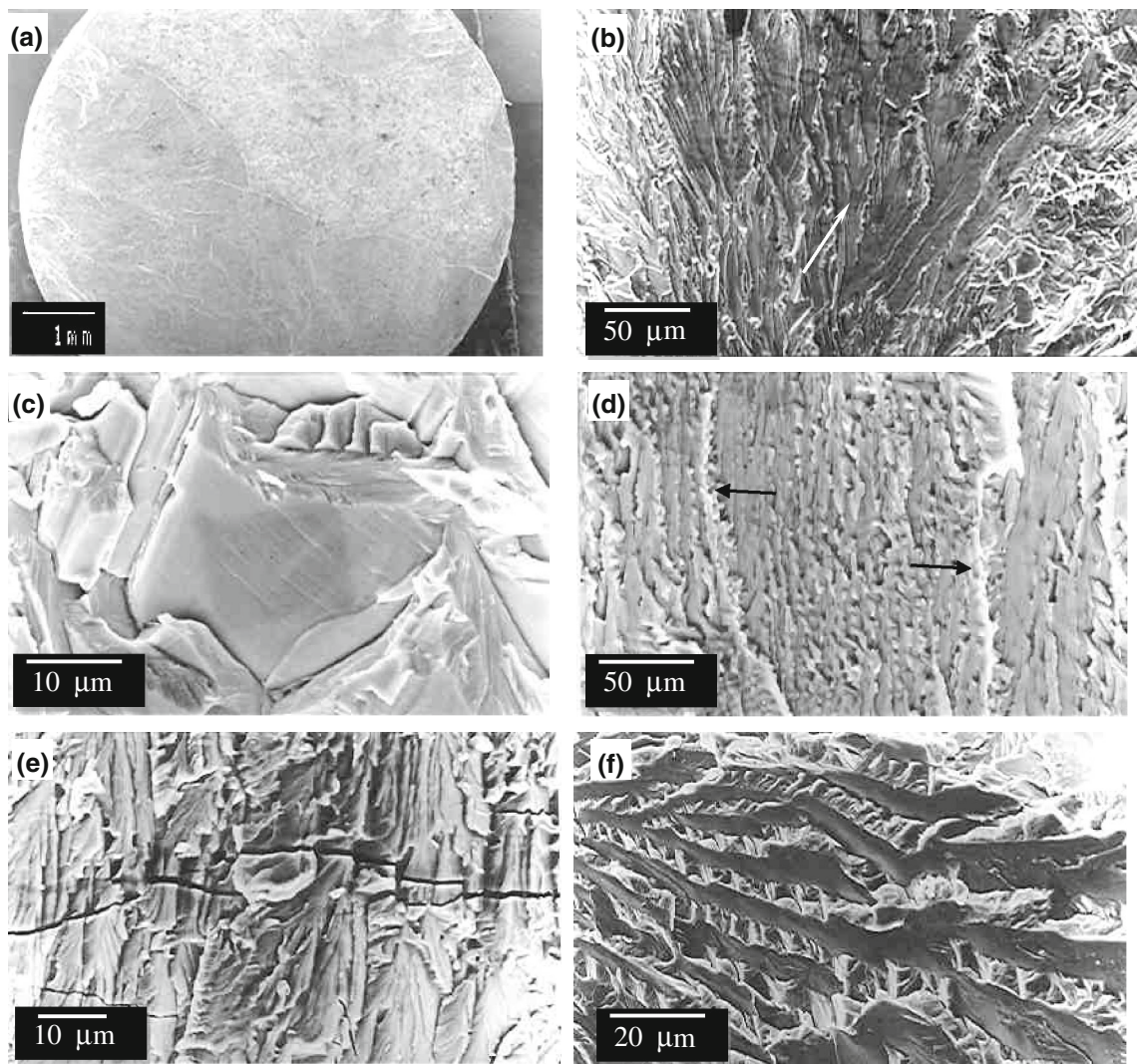


Fig. 7—Fracture surfaces showing: (a) macroscopically flat fracture, (b) river patterns, (c) facet planes, (d) cleavage steps, (e) crack propagation path, and (f) plastic deformation of the αV lamella.

material. In addition, the ductile reinforcement can promote the process of transfer slip ductile brittle phase to phase and can relieve the stress concentration at the interface, thereby contributing to toughening. The toughness value obtained in this work is larger than the monocrystalline and polycrystalline NiAl as well as all the NiAl-based eutectics (Table III), making it one of the toughest materials of this class. The increased toughness compared to NiAl has been attributed to the presence of the ductile phase as well as to its high volume fraction.

Important information about the nature of the fracture can be obtained by microscopic examination of the fracture surface. Detailed analysis of the fracture surface in order to determine the cause of the fracture and the relationship between microstructure and fracture mode of the material has been performed. Figures 7(a) and (b) show transverse fracture surfaces of samples directionally solidified after the bending tests. In these figures, it is noted clearly that the fracture surface is flat and of transgranular type. The surface was characterized by flat facets, as shown in Figure 7(c). Furthermore, the cleavage steps and river patterns, which present a change in the plane of the crack propagation and are the main characteristics of brittle fracture by cleavage were observed (arrows in Figure 7(d)). All this indicated that the micromechanism of fracture was cleavage, since the material ductility is not sufficient for the formation of dimples.

Figure 7(e) shows the crack propagation features typical for transgranular type of fracture. The cracks developed by discontinuous segments along a preferential cleavage planes. Crack initiation occurred mainly in the NiAl matrix, but the crack propagation was retarded by the ductile vanadium lamellae. Subsequent crack growth, therefore, involved the re-initiation of cracks in the adjacent interfacial lamellae. Furthermore, it can be seen that when it reaches a new phase, a crack undergoes a small change in direction. This small change of direction means that each lamella is an obstacle to crack propagation and the greater the number of obstacles to the crack propagation, the higher toughness of the alloy.^[30] According to Heredia *et al.*^[9] in microstructures with alternating layers of brittle and ductile phases, the crack propagation can be impeded by crack tip blunting mechanism or the formation of cracks at the interface which undergoes phase separation. In both cases, the more ductile layer modifies the stress ahead of the crack. As it can be seen in Figure 7(f), the rougher V phase was much more deformed before the fracture, than the NiAl phase. Also, although the vanadium lamellae were deformed plastically, none of them were observed to fracture during the crack development and fractured only at the onset of catastrophic failure.

IV. SUMMARY

The mechanical properties and fracture behavior of directionally solidified NiAl-V eutectic composite have been investigated and the results can be summarized as follows:

1. Compression tests showed that the eutectic NiAl-V exhibits higher yield strength and ductility than the majority of single crystals and polycrystals of NiAl. At higher temperatures, a steep drop with increasing temperature, attributed to ductile/brittle transition was observed.
2. The microhardness results indicate that the both constituent phases were significantly solution hardened. Also, the composite in the form of a eutectic alloy exhibited a balance of hardness of the constituent phases.
3. The fracture toughness, K_{IC} , of the NiAl-V *in situ* composite was $28.6 \pm 0.3 \text{ MPa}\sqrt{\text{m}}$. Despite showing a slightly lower value to literature data, the same is greater than the toughness of NiAl in the form of single crystals and polycrystals as well as the most NiAl-based eutectics, which makes it one of the toughest materials of this class. The increased toughness compared to NiAl is due to the presence of the ductile phase, which also serves as a barrier to crack propagation.
4. The analysis of the fracture surface of the composite *in situ* NiAl-V indicated that the material exhibits macroscopically flat fracture surface. Regarding the microscopic aspects, the material exhibited brittle fracture behavior of transgranular type. Finally, all observations pointed out that the main fracture micromechanism was cleavage.

ACKNOWLEDGMENTS

Funding of the Project NECTAR (PCIG10-GA-2011-303409) by the Marie Curie Actions Grant FP7-PEOPLE-2011-CIG program is gratefully acknowledged. SM acknowledges the Ramon y Cajal fellowships from the Spanish Ministry of Economy and Competitiveness. The financial support from the São Paulo State Research Foundation (FAPESP, Brazil) is acknowledged.

REFERENCES

1. D.B. Miracle: *Acta Metall. Mater.*, 1993, vol. 41, pp. 649–84.
2. R.D. Noebe, R.R. Bowman, and M. Nathal: *Int. Mater. Rev.*, 1993, vol. 38, pp. 193–231.
3. A. Misra and R. Gibala: *Metall. Mater. Trans. A*, 1997, vol. 28A, pp. 795–807.
4. M.G. Mendiratta, J.J. Levandowski, and D.M. Dimiduk: *Metall. Trans. A*, 1991, vol. 22A, pp. 1573–83.
5. G. Frommeyer, R. Rosenkranz, and C. Ludecke: *Zeit. Metallkd.*, 1991, vol. 81, pp. 307–13.
6. J.D. Whittenberger, R.D. Noebe, D.R. Johnson, and B.F. Oliver: *Intermetallics*, 1997, vol. 5, pp. 173–83.
7. D.T. Jiang and J.T. Guo: *Mater. Sci. Eng. A*, 1998, vol. 225, p. 154.
8. J.T. Guo, C.Y. Cui, Y.X. Chen, D.X. Li, and H.Q. Ye: *Intermetallics*, 2001, vol. 9, pp. 287–97.
9. F.E. Heredia, M.Y. He, G.E. Lucas, A.G. Evans, and H.E. Dève: *Acta Metall. Mater.*, 1993, vol. 41, pp. 505–11.
10. P.R. Subramanian, M.G. Mendiratta, and D.B. Miracle: *Metall. Mater. Trans. A*, 1994, vol. 25A, pp. 2769–81.
11. A. Misra, R. Gibala, and R.D. Noebe: *Intermetallics*, 2001, vol. 9, pp. 971–8.

12. C.Y. Cui, J.T. Guo, Y.H. Qi, and H.Q. Ye: *Mater. Sci. Eng. A*, 2004, vol. 385, pp. 359–66.
13. H. Bei and E.P. George: *Acta Mater.*, 2005, vol. 53, pp. 69–77.
14. B. Zeumert and G. Sauthoff: *Intermetallics*, 1997, vol. 5, pp. 563–77.
15. P.L. Ferrandini, F.L.G.U. Araujo, W.W. Batista, and R. Caram: *J. Cryst. Growth*, 2005, vol. 275, pp. 147–52.
16. P.W. Pellegrini and J.J. Huta: *J. Cryst. Growth*, 1977, vol. 42, pp. 536–39.
17. J.D. Cotton and M.J. Kaufman: *Scripta Metall. Mater.*, 1991, vol. 25, pp. 1827–36.
18. S.M. Joslin, X.F. Chen, B.F. Oliver, and R.D. Noebe: *Mater. Sci. Eng. A*, 1995, vol. 196, pp. 9–18.
19. S. Milenkovic, A.A. Coelho, and R. Caram: *J. Cryst. Growth*, 2000, vol. 211, pp. 485–90.
20. S. Milenkovic and R. Caram: *Mater. Lett.*, 2002, vol. 55, pp. 126–31.
21. S. Milenkovic and R. Caram: *J. Mater. Proc. Technol.*, 2003, vols. 143–144, pp. 629–35.
22. J.D. Hunt and K.A. Jackson: *Trans. Met. Soc. AIME*, 1966, vol. 236, pp. 843–52.
23. J.D. Hunt and J.P. Chilton: *J. Inst. Met.*, 1962, vol. 91, pp. 338–45.
24. R. Darolia: *J. Met.*, 1991, vol. 43, pp. 44–49.
25. J.L. Walter and H.E. Cline: *Metall. Trans.*, 1970, vol. 1, pp. 1221–29.
26. G. Frommeyer and R. Rablbauer, *MRS Proc.*, 2002, vol. 753, BB4.6.
27. D.R. Johnson, S.M. Joslin, B.F. Oliver, R.D. Noebe, and J.D. Whittenberger: *Intermetallics*, 1995, vol. 3, pp. 99–113.
28. P.R. Subramanian, M.G. Mendiratta, D.B. Miracle, and D.M. Dimiduk: in *MRS Symposium on Intermetallic Matrix Composites II*, 1990, vol. 194, pp. 147–54.
29. *Annual Book of ASTM Standards: "Standard Test Method for Plane-Strain Fracture Toughness of Metallic Materials"*: E-399-90, ASTM, Philadelphia, PA, 1991, vol. 03.01, p. 485.
30. R.W. Hertzberg: *Deformation and Fracture Mechanics of Engineering Solids*, 4th ed., Wiley, New York, 1996, pp. 164–201.